On Mixing by Trade-Wind Cumuli

HOWARD P. HANSON[1]

Cooperative Institute for Marine and Atmospheric Studies, University of Miami/NOAA, Miami, FL 33149

(Manuscript received 10 June 1980, in final form 12 January 1981)

ABSTRACT

Mixing processes associated with tropical marine boundary-layer cumuli are examined with a one-dimensional, steady-state model of the cloud and inversion layers which explicitly differentiates between cloud-scale and subcloud-scale motions. Physically, the clouds are modeled as an ensemble average of well-mixed turbulent bursts into an otherwise quiescent, subsiding environment. The cloud-base vertical velocity distribution is found from a new closure based on a simplified vertical momentum budget. The clouds are described by two free parameters, fractional area and a detrainment time scale.

Faster detrainment rates are shown to be associated with undiluted clouds, in the sense that the cloud entrainment rate becomes zero. For this case, the cloud-scale fluxes dominate the boundary-layer mixing. Conversely, slower detrainment and large entrainment imply a diluted cloud, with the boundary-layer mixing dominated by the subcloud-scale turbulence.

Simple qualitative arguments show that the vertically averaged temperature perturbation of the clouds is very small and that increases in cloud-base moist static energy fluxes lead to enhancement of the cloud-top entrainment instability and vertical mixing associated with increasingly larger scales.

1. Introduction

The tropical and subtropical oceans cover some 37% of the earth's surface and are responsible for nearly half of the solar energy absorbed by the entire planet. Somewhat more than half of this energy is transferred to the tropical atmosphere, largely by surface latent heat fluxes, and is ultimately released in tropical disturbances, both transient and stationary (e.g., the intertropical convergence zone; Riehl and Simpson, 1979). These disturbed areas cover a small fraction of the tropical oceans, the remainder of which are overlain by the undisturbed trades. The undisturbed trade-wind planetary boundary layer (PBL) acts as a collector of heat and moisture for the disturbances, and the processes taking place in the PBL therefore determine the amount of energy available to drive the tropical circulation. In an idealized sense (e.g., Arakawa, 1975), the tradewind PBL undergoes a transition from the upstream coastal stratocumulus regimes to the fair-weather, nearly clear trade-wind cumulus regimes along low-level trajectories. This paper concerns the vertical mixing of heat and moisture associated with these various regimes of suppressed clouds.

Beyond their role in mixing heat and moisture into the lower atmosphere, trade-wind PBL clouds, having much higher albedos than the ocean surface, strongly affect the absorption of solar energy by the oceans. This is especially true across the transition from the stratocumulus to the trade cumulus regimes, where the albedo can decrease by a factor of 2 (e.g., Winston *et al.*, 1979). Overall, the current research effort concerns the variation of the ocean-surface energy balance as these cloud regimes change along the trade winds. This paper concentrates on one part of this, modeling the processes of trade cumulus cloud mixing. One aspect of this left unresolved here is the cloud entrainment rate; it is felt that the classical approach used by, for example, Arakawa and Schubert (1974) is inadequate to describe the various closed and open convection regimes observed across the transition.

Diagnostic model studies of tropical cloud populations (e.g., Nitta, 1975; Yanai *et al.*, 1976) in both the undisturbed and the disturbed troposphere have shown that the role of trade-wind PBL cloud processes is to cool and moisten the upper part of the PBL, thereby maintaining the trade-wind inversion and providing a moist environment for the deeper clouds. Although seldom associated with disturbances, clouds in the stratocumulus regime also behave in this manner (e.g., Schubert *et al.*, 1979). The physical mechanisms of these processes are different for stratocumulus and trade cumulus, however. In the former all scales of motions occur in saturated conditions, while in the latter, there are motions associated with both saturated and unsaturated conditions. Although the diagnostic models

[1] National Research Council Resident Research Associate, Atlantic Oceanographic and Meteorological Laboratory, NOAA.

0022-4928/81/051003-12$07.00

implicitly compute the effects of all subgrid-scale fluxes, predictive models of trade cumulus have included only the scales associated with the saturated updrafts and unsaturated compensating downdrafts. This may be shown as follows.

If σ represents the fractional cloud area and h represents a field variable in the layer (here, it will be moist static energy), a large-scale average can be decomposed into cloud and environmental averages:

$$\bar{h} = \sigma \bar{h}^c + (1 - \sigma)\bar{h}^e. \tag{1a}$$

Vertical fluxes involve quadratic terms (Esbensen, 1978; Augstein *et al.*, 1979) and [using w for vertical velocity and primes for departures from the respective averages; e.g., $\overline{w'h'}^c \equiv \overline{(w - \bar{w}^c)(h - \bar{h}^c)}^c$]

$$\overline{w'h'} = \sigma\overline{w'h'}^c + (1 - \sigma)\overline{w'h'}^e$$

$$\text{(i)} \qquad \text{(ii)}$$

$$+ \sigma(1 - \sigma)(\bar{w}^c - \bar{w}^e)(\bar{h}^c - \bar{h}^e). \tag{1b}$$

$$\text{(iii)}$$

Previous studies of trade-wind cumulus (e.g., Betts, 1973, 1975; Esbensen, 1978; Albrecht *et al.*, 1979) have concentrated on term (iii) above as the mechanism whereby the clouds effect vertical mixing. [Esbensen (1978) included term (ii) to calculate fluxes by buoyant clouds, which penetrate into the trade-wind inversion and appear in the "environment" of the subinversion clouds in which he was interested.] Term (iii) represents the subgrid-scale fluxes due to cloud-mean (saturated) updrafts and environmental (unsaturated) downdrafts; this will be called "overturning" below. A further simplification employed in trade cumulus models takes $\sigma \ll 1$; this is clearly invalid for much of the undisturbed trade PBL. The stratocumulus models, of course, are concerned with term (i) exclusively. Albrecht (1979) adapted the trade cumulus model for stratocumulus conditions employing term (iii) only, by assuming that $\bar{h}^e$ was saturated and that the $(1 - \sigma)$ factor was unimportant. His results compared favorably with the previous stratocumulus modeling efforts (using term i) despite the inconsistency.

In the research reported here, the processes represented by terms (i) and (iii) are included in a simplified, vertically integrated, quasi-one-dimensional model of the cloud and inversion layers. Term (ii) is ignored since observations (LeMone and Pennell, 1976; Warner, 1977) show that the environmental turbulence is much less than that in the clouds. The assumption that $\sigma \ll 1$ is avoided. Section 2 contains the model budget assumptions and development; the results reduce analytically to the stratocumulus model first discussed by Lilly (1968). For cases of partial cloud coverage, it is necessary to find the cloud-base vertical velocity distribution—a classic problem in cloud modeling—and this is derived in Section 3 from a vertical circulation integral of the cloud-environment buoyancy forcing. The focus of this paper concerns the interplay of terms (i) and (iii) in (1b), and no attempt is made to include the surface, subcloud and transition layers. Therefore, the results discussed in Section 4 are obtained by specifying the layer geometry and cloud-base-level subgrid fluxes of heat and moisture. Because of the overall scope of this research discussed above the entrainment rate is not parameterized, but varied as a free parameter. The conditions used here, from the Atlantic Trade Wind Experiment (ATEX), represent an extreme case which strains the model assumptions, but provides a clear delineation of the mixing effects of terms (i) and (iii) in (1b). This is discussed in Section 5.

2. Budgets

Since they are conservative with respect to water phase changes, the budget variables used here are total water,

$$r = q + l,$$

where q and l are specific humidities of water vapor and liquid, and moist static energy,

$$h = c_p T + Lq + gz,$$

where T is temperature, z is height, and c_p, L and g are the specific heat of air (at constant pressure), the latent heat of vaporization and gravitational acceleration. The moist static energy budget is simply

$$\frac{dh}{dt} = -\frac{1}{\rho}\frac{\partial F_R}{\partial z}, \tag{2}$$

where $d/dt = \partial/\partial t + \mathbf{V}\cdot\nabla + w\partial/\partial z$ and F_R is the upward flux of radiation; $\mathbf{V}$ is the horizontal velocity vector, ∇ the horizontal gradient operator, ρ is density and t is time. The total water budget is similar to (2) with F_R replaced by F_P, the precipitation flux. Only the moist static energy budget is treated here, since the total water budget follows exactly analogously. A third possible choice of a conservative variable is the liquid static energy, $s_l = h - Lr$ (Betts, 1973; Deardorff, 1976b). This is not used in a predictive sense here because the precipitation flux divergence would then appear in both the s_l and r equations; however, in some of the results below, the modeled processes are interpreted in terms of s_l because it is equal to the dry static energy in the environment, where $l = 0$, and this simplifies the discussion.

Shallow (below ~2 km) clouds are modeled exclusively in this study; thus the incompressible assumption will be used for the great simplicity it offers:

$$\nabla\cdot\mathbf{V} + \partial w/\partial z = 0. \tag{3a}$$

The large-scale average of (3a) is

$$\overline{\nabla \cdot \mathbf{V}} \equiv \bar{D} = -\partial \bar{w}/\partial z. \tag{3b}$$

Applying (3a) to (2) and using (3b) gives the large-scale budget:

$$\frac{\partial \bar{h}}{\partial t} + \bar{\mathbf{V}} \cdot \overline{\nabla h} + \overline{\nabla \cdot \mathbf{V}' h'} + \bar{w} \frac{\partial \bar{h}}{\partial z} + \frac{\partial}{\partial z} \overline{w' h'} = -\frac{1}{\rho} \frac{\partial \bar{F}_R}{\partial z}. \tag{4}$$

The fifth term in (4) is given by (1b). To simplify the model, $\bar{D}$, $\partial \bar{F}_R/\partial z$ and $\bar{\mathbf{V}} \cdot \overline{\nabla h}$ are assumed constant with height, and it is also assumed that the large-scale advection affects clouds and environment identically. These assumptions are common in vertically integrated, one-dimensional models, and are justified by the separation of time scales between modeled cloud processes and large-scale processes (Yanai *et al.*, 1976). The divergence of the horizontal eddy fluxes $\overline{\nabla \cdot \mathbf{V}' h'}$ is ignored in this study of the undisturbed trades.

Defining a large-scale forcing

$$\overline{G_h} = \bar{\mathbf{V}} \cdot \overline{\nabla h} + \frac{1}{\rho} \frac{\partial \bar{F}_R}{\partial z},$$

the large-scale budget becomes

$$\frac{\partial \bar{h}}{\partial t} + \bar{w} \frac{\partial \bar{h}}{\partial z} + \frac{\partial}{\partial z} \overline{w' h'} = -\overline{G_h}. \tag{5}$$

In diagnostic studies (e.g., Yanai *et al.*, 1973), the first two terms are lumped together with the forcing; here, the large-scale vertical structure is a dependent variable. Since the divergence is constant with height and the vertical velocity must vanish at the ocean surface,

$$\bar{w} = -\bar{D}z. \tag{6}$$

Defining forcing for the clouds as

$$\bar{G}_h^c \equiv \bar{\mathbf{V}} \cdot \overline{\nabla h} + \frac{1}{\rho} \frac{\partial \bar{F}_R^c}{\partial z},$$

the cloud-averaged budget is

$$\frac{\partial \bar{h}^c}{\partial t} + \bar{w}^c \frac{\partial \bar{h}^c}{\partial z} + \frac{\partial}{\partial z} \overline{w' h'}^c + \bar{E}^c (\bar{h}^c - \bar{h}^e) = -\bar{G}_h^c. \tag{7}$$

The entrainment (fourth) term arises from a horizontal circulation integral around the cloud of the cloud-averaged horizontal eddy flux divergence. It is useful to note that if the vertical advection (second) term were written in flux form the entrainment term would become $(\bar{D}^c \bar{h}^c - \bar{E}^c \bar{h}^e)$ where $\bar{D}^c$ represents cloud detrainment (Ooyama, 1971).

The horizontal terms of the environmental budget can be deduced from the large-scale and cloud budgets, with (1b), (6) and (7), and

$$\frac{\partial \bar{h}^e}{\partial t} + \bar{w}^e \frac{\partial \bar{h}^e}{\partial z} + \frac{\partial}{\partial z} \overline{w' h'}^e - \frac{\sigma}{1-\sigma} (\bar{D}^c - \bar{D})(\bar{h}^c - \bar{h}^e) = -\bar{G}_h^e, \tag{8}$$

where

$$\bar{G}_h^e \equiv \bar{\mathbf{V}} \cdot \overline{\nabla h} + \frac{1}{\rho} \frac{\partial \bar{F}_R^e}{\partial z}.$$

[Multiplying (7) by σ and (8) by $(1 - \sigma)$, and adding, gives (5).] Eqs. (7) and (8) are now to be simplified and solved analytically.

The budget equations (7) and (8) express a balance among storage, vertical advection, vertical mixing and lateral exchange between the clouds and the environment as a function of the large-scale advective and radiative forcing for the clouds and the environment, respectively. Averaged over all clear areas, the environment responds to the presence of the clouds through detrainment by evaporating clouds and enhanced subsidence (i.e., $|\bar{w}^e| > |\bar{w}|$) in compensation for the cloud updrafts. The clouds are affected by the environment through the entrainment term and the cloud-environment buoyancy-driven cloud updrafts. For this analysis, the interest is on the balances which act to maintain the vertical structure of the cloud and inversion layers; accordingly, the steady state is examined and the storage (first) terms in (7) and (8) are dropped. As discussed in the Introduction, the small-scale environmental turbulence [third term in (8)] is ignored compared to the in-cloud turbulence and the saturated updraft-dry downdraft circulation.

Simplifying the cloud-averaged budget equation is less straightforward, because it contains both the mean and turbulent contributions to the in-cloud vertical flux of h. There is a hierarchy of turbulence closure parameterization techniques available for relating $\overline{w'h'}^c$ to $\bar{h}^c$; they have been reviewed, for the upper ocean, by Niiler and Kraus (1977). The zero-order approach is the application of a mixed-layer hypothesis, wherein the mean field (in this case $\bar{h}^c$) is assumed to be vertically well-mixed, and the turbulent fluxes are therefore required to be linear, in the absence of other processes, to maintain this well-mixed state. For mixed-layer models, the mean vertical advection is zero (since, here, $\partial \bar{h}^c/\partial z = 0$). The undisturbed trade-wind PBL model of Albrecht *et al.* (1979) employs what may be termed a "half-order" approach; they assumed the mean quantities to be linear with height and the turbulent fluxes [using only term (iii) in (1b)] to be quadratic. The first-order closure is simply the classical mixing-length hypothesis, wherein the turbulent fluxes are proportional to the first derivative of the mean-field quantities. Higher orders involve solving the moment

equations more-or-less explicitly (e.g., Mellor and Yamada, 1974).

In this paper, the well-mixed approach is used because it represents the simplest possible closure to find $\overline{w'h'}^c$; this is consistent with the other simplified assumptions adopted. The first-order closure has two disadvantages: a mixing length must be specified, which would not necessarily be empirically well-defined for all the cloud-types of interest here; and the budget equations (7) and (8) reduce to a rather cumbersome third-order differential equation with linear coefficients. (It will be seen below that the well-mixed approach yields first-order equations.) The main disadvantage of the well-mixed closure is that it overpredicts the mixing by the small-scale turbulence for trade cumulus conditions. This is straightforward to understand: in a horizontally uniform large-scale averaging area, the trade cumulus cloud population consists of a large number of inactive, decaying clouds and considerably fewer actively growing clouds (during ATEX, Augstein *et al.*, 1973, estimated that only ~2% of the clouds were active). For steady-state conditions, there is a growth/decay equilibrium, with "new" clouds occurring at a rate which balances the evaporation of "old" ones. While the growing clouds may perhaps be realistically modeled as well mixed, the decaying clouds are not well mixed, and by averaging over all clouds—as is done in (1)—this assumption places too much emphasis on the small-scale turbulence.

A better approach would be to have three averaging subdomains—active clouds, inactive clouds and the environment, with only active clouds associated with subcloud-scale turbulence (i.e., $\overline{w'h'}^c$-type fluxes). The active clouds would be converted to decaying clouds, and the latter would perform the detrainment process: entrainment would be associated only with the growing clouds. This would introduce at least two more parameters. Under the present assumptions, that all the clouds are averaged together, both of these processes appear in the cloud-averaged continuity equation

$$\overline{\nabla\cdot\mathbf{V}}^c = \bar{D}^c - \bar{E}^c = -\partial\bar{w}^c/\partial z, \tag{9}$$

where $\bar{D}^c$ is the time scale for cloud detrainment and $\bar{E}^c$ is the time scale for (lateral) cloud entrainment. It is assumed here that $\bar{D}^c$ and $\bar{E}^c$ are each constant with height; this makes the cloud updrafts $\bar{w}^c$ linear. Esbensen's (1978) low-cloud model does not make this assumption; his results (Fig. 11) indicate that the entrainment and detrainment are nearly constant with height except near cloud base. It is further assumed that the fractional cloud area is constant with height.

The assumptions discussed above represent a consistent lowest order approach which can be used to investigate the effects of cloud-related mixing on the layer structure and the roles of the two processes represented by terms (i) and (iii) in (1b). They lead to the budget equations

$$\frac{\partial}{\partial z}\overline{w'h'}^c + \bar{E}^c(\bar{h}^c - \bar{h}^e) = -\bar{G}_h^c, \tag{10a}$$

$$\bar{w}^e\frac{\partial\bar{h}^e}{\partial z} - \bar{D}\mu(\bar{h}^c - \bar{h}^e) = -\bar{G}_h^e, \tag{10b}$$

where

$$\mu \equiv \frac{\sigma}{1-\sigma}\left(\frac{\bar{D}^c}{\bar{D}} - 1\right)$$

represents the rate of environmental dilution by the clouds normalized by the large-scale divergence. The cloud budget is thus a balance of small-scale turbulent flux divergence, entrainment and large-scale forcing by radiation and advection. The environmental budget is a balance of environment-mean vertical advection, cloud entrainment and large-scale forcing. (Except for radiation effects, $\bar{G}_h^e$ and $\bar{G}_h^c$ are identical.) Physically, then, the clouds are taken here to be well-mixed turbulent bursts which entrain upward and laterally into an otherwise quiescent, subsiding, stratified layer then dilute the layer by evaporation during detrainment.

Unlike spectral cloud models (e.g., Arakawa and Schubert, 1974), this model has no thin detrainment layers, and the vertical velocity structure must be (piecewise) continuous; this implies that at the top of the PBL ($z = z_B$),

$$\bar{w}_B = \bar{w}_B^e = \bar{w}_B^c.$$

It is convenient to define a nondimensional measure of the cloud-base ($z = z_C$) velocities as

$$\alpha \equiv \bar{w}_C^e/\bar{w}_B,$$

using this, the linear structure of $\bar{w}$ and (1a),

$$\bar{w}_C^c = -\frac{\bar{w}_B}{\sigma}[(1-\sigma)\alpha - z_C/z_B].$$

This definition is useful because $\alpha \geq z_C/z_B$ (i.e., $\bar{w}_C^e \leq \bar{w}_C$) since the overturning must consist of the clouds rising with respect to the environment. (If the environment were to rise, it would condense into a cloud.) Another useful definition is a nondimensional height in the cloud/inversion layers, i.e.,

$$\hat{z} \equiv (z - z_C)/(z_B - z_C).$$

Finally, by defining a cloud-environment difference of moist static energy, $\Delta h(\hat{z}) \equiv \bar{h}^c - \bar{h}^e(\hat{z})$, (10b) becomes

$$[\alpha + (1-\alpha)\hat{z}]\frac{d\Delta h}{d\hat{z}} - \mu(1 - z_C/z_B)\Delta h = -(\bar{G}_h^e/\bar{D})(1 - z_C/z_B). \tag{11a}$$

Now, at the cloud tops, the small-scale turbulence,

$\overline{w'h'}^c_B$, is included to allow entrainment into the upper air as in stratocumulus-topped mixed layer models (Lilly, 1968; Schubert *et al.*, 1979); it is this mechanism which maintains the PBL against subsidence from above. In the environment, however, no such mechanism exists in this model, since $\overline{w'h'}^e$ has been neglected altogether. Thus, the troposphere subsides unmodified into the top of the PBL between the clouds, and the appropriate boundary condition for (11a) is

$$\Delta h_B = \bar{h}^c - \bar{h}^e_B = \bar{h}^c - h_u, \qquad (11b)$$

where h_u is specified from profiles of T and q above the PBL. Near the cloud tops, then, the *lateral* entrainment, at a rate $\bar{E}^c$, occurs at the same cloud-environment difference as the *upward* entrainment (into the subsiding air), represented by $\overline{w'h'}^c_B$.

With this preparation, the environment budget (11) can be solved analytically, and

$$\Delta h(\hat{z}) = \Delta h_B f(\hat{z}) + \bar{G}^e_h/(\bar{D}\mu)[1 - f(\hat{z})], \qquad (12a)$$

where the vertical structure is governed by

$$f(\hat{z}) = [\alpha + (1-\alpha)\hat{z}] \times [\alpha + (1-\alpha)\hat{z}]^{[\mu(1-z_C/z_B)/(1-\alpha)]}. \qquad (12b)$$

Curves of $f(\hat{z})$ are shown in Fig. 1, for $z_C/z_B = 0.25$. Physically, these may be interpreted as environmental liquid static energy profiles, normalized by $\Delta s_{l_B} = \Delta h_B - L\Delta r_B$, obtained by neglecting radiation and advection. The left sides of the panels correspond to $\bar{s}^c_l$ and the right sides to $s_{l_u} = \bar{s}^e_l(z_B)$. In Fig. 1a the overturning is neglected ($\alpha = z_C/z_B$) and the parameter μ is varied. As μ increases, the dilution of the environment by detraining clouds strengthens the environmental inversion and causes the lower part of the layer to become more nearly horizontally well-mixed. For small values of μ, the downward advection dominates the detrainment and the inversion disappears. From this it is seen that the trade-wind inversion is produced by detraining clouds (Betts, 1975).

Fig. 1b shows curves of $f(\hat{z})$ for $\mu = 5$ and various amounts of overturning as measured by α. Near the top of the layer, the overturning has little effect; lower down, however, it increases $f(\hat{z})$ because of enhanced downward advection. This has the effect of sharpening the environmental inversion. In Section 3 an expression will be derived which will allow α to be calculated from the thermodynamic profiles.

Using Eqs. (12), the in-cloud budget (10a) can be directly integrated to give

$$\overline{w'h'}^c_B - \overline{w'h'}^c_C + \bar{E}^c(z_B - z_C)\left[\Delta h_B\left(\frac{1-g_C}{\mu'}\right) + \bar{G}^e_h/(\bar{D}\mu)\left(1 - \frac{1-g_C}{\mu'}\right)\right] = -\bar{G}^c_h(z_B - z_C), \qquad (13a)$$

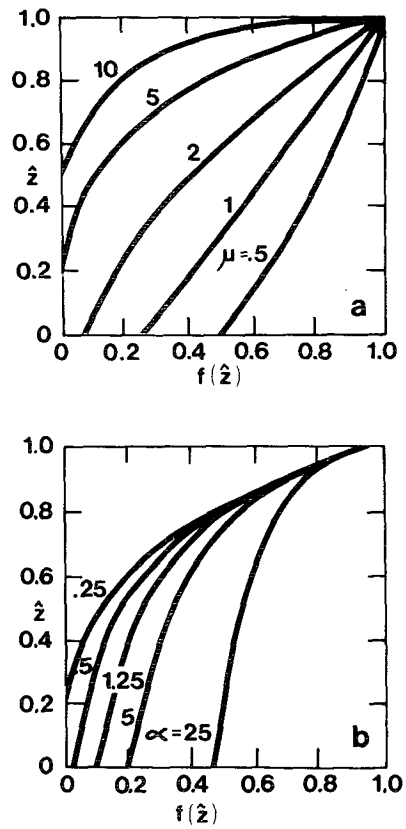

FIG. 1. Vertical structure function, $f(\hat{z})$ versus nondimensional height ($\hat{z}$) for (a) no overturning and various rates of environmental dilution μ, and (b) for $\mu = 5.0$ and various rates of overturning (α). In each part $z_C/z_B = 0.25$.

where the integral of $f(\hat{z})$ [$=g(\hat{z})/\mu'$ + constant] involves

$$g(\hat{z}) \equiv [\alpha + (1-\alpha)\hat{z}]^{[\mu(1-z_C/z_B)/(1-\alpha)+1]}, \qquad (13b)$$

$$\mu' \equiv \mu(1 - z_C/z_B) + (1-\alpha). \qquad (13c)$$

Since the clouds have been assumed to be vertically well-mixed, the small-scale turbulent flux must be

$$\overline{w'h'}^c(\hat{z}) = \overline{w'h'}^c_C(1-\hat{z}) + \overline{w'h'}^c_B\hat{z} + \bar{E}^c(z_B - z_C) \times [\Delta h_B - \bar{G}^e_h/(\bar{D}\mu)]\left\{\frac{\hat{z}(1-g_C) - [g(\hat{z}) - g_C]}{\mu'}\right\}. \qquad (14)$$

The last term represents the flux required to keep the clouds well-mixed in the face of entrainment of the nonuniform environment.

The cloud-base flux is found from (1b):

$$\overline{w'h'}^c_C = \frac{\overline{w'h'}_C}{\sigma} - (1-\sigma)(\bar{w}^c_C - \bar{w}^e_C)\Delta h_C, \qquad (15a)$$

where $\overline{w'h'}_C$ must be specified in the absence of subcloud and transition layer models. Cloud-top entrainment is governed by (Lilly, 1968):

$$\overline{w'h'}^c_B = -\bar{w}_B\Delta h_B + \rho^{-1}\Delta F^{cl}_R \qquad (15b)$$

where $\Delta F_R^{c\prime}$ is the prescribed cloud-top jump of radiative flux. Although a more detailed description of this is desirable (Deardorff, 1976a; Kahn and Businger, 1979; Schubert *et al.*, 1979; Randall, 1980b) the simple jump formulation used here is not critical to the analysis since the turbulence energy equation is not included (Deardorff and Businger, 1980; Lilly and Schubert, 1980).

The in-cloud moist static energy can now be found from (11b), (12a, b), (13a, b, c), (14) and (15a, b):

$$\Delta h_B = \frac{\overline{w'h'}_C/\sigma - G_h'}{\omega_u}, \tag{16a}$$

where

$$\omega_u \equiv -\left\{\bar{w}_B - (1-\sigma)(\bar{w}_C^c - \bar{w}_C^e)f_C - \bar{E}^c(z_B - z_C)\left[\frac{1-g_C}{\mu'}\right]\right\} \tag{16b}$$

is the net input rate to the clouds from the top and sides, and

$$G_h' \equiv \rho^{-1}\Delta F_R^{c\prime} + \bar{G}_h^c(z_B - z_C) + \bar{G}_h^e/(\bar{D}\mu) \times \{(1-\sigma)(\bar{w}_C^c - \bar{w}_C^e)(1-f_C) + \bar{E}^c(z_B - z_C)[1 - \mu^{-1}(1-g_C)]\} \tag{16c}$$

is the net effect of radiation and advection on the clouds. This model is limited to describing the mixing processes in the cloud/inversion layers; a complete PBL model would also find z_B, z_C and $\overline{w'h'}_C$, and the two cloud parameters, σ and $\bar{D}^c$, which must all be specified here.

In the stratocumulus limit ($\sigma \to 1$) the environmental dilution rate μ becomes infinite unless the detrainment rate becomes equal to the large-scale divergence. Hence it is required that, in the limit $\sigma \to 1$, $(\bar{D}^c - \bar{D})/(1-\sigma) = 1$. This makes physical sense because as the environment disappears, the cloud "detrainment" is out the sides of the large-scale averaging domain, and must equal the large-scale divergence. In this limit, the cloud entrainment and overturning vanish, of course, and the environment budget equations (12a, b) become superfluous. The cloud budget equations [(13a) and (14)] and the cloud-top inversion strength (16a, b, c) all reduce to the one-dimensional stratocumulus model. The weighted-average form of (16a) has been discussed by Schubert (1976), who also included the surface and subcloud layers.

Eqs. (16) offer a useful qualitative insight into the behavior of the trade-wind PBL. The large-scale vertical motion is downward, the overturning is one-way ($\bar{w}_C^c > \bar{w}_C^e$) and the entrainment is positive, so ω_u is positive definite. Radiative cooling and positive downstream advection (upgradient) cause $G_h' > 0$. Cloud-base fluxes and internal sinks therefore have opposing influences on the strength of the cloud-top inversion, $-\Delta h_B = h_u - \bar{h}^c$. Lilly (1968) asserted that the stability of a stratocumulus deck requires $-\Delta h_B > 0$, so that entrained parcels would remain buoyant with respect to the cloud tops while they became saturated. Randall (1980a) and Deardorff (1980) have shown that correcting for liquid water loading allows stability for small negative values of $(-\Delta h_B)$, but Lilly's (1968) criterion remains qualitatively valid. Clearly, (16a) shows that increased cloud-base fluxes lead to enhancement of the cloud-top entrainment instability (Deardorff, 1980); i.e., they destabilize not only a stratocumulus deck but increase the instability for partly cloudy conditions.

It should also be noted that the opposing effects of cloud-base fluxes and large-scale sinks on the inversion strength imply an adjustment by the atmosphere to some balance which, in general, is likely to be nonzero. Any model which requires Δh_B, Δr_B or any combination thereof to vanish [e.g., the Arakawa and Schubert (1974) spectral model, or Esbensen's (1978) low-cloud model] implicitly constrains this adjustment. The effects of this constraint on the behavior of such models remain untested.

3. Overturning

The assumptions introduced above imply that the vertical velocities are linear with height and known at the PBL top, z_B. The cloud-base velocities, and thus the overturning strength, are yet to be determined. This is accomplished with a vertically integrated vertical momentum balance using a simplified form of the vertical momentum equation:

$$\frac{dw}{dt} = g\frac{s_v - \bar{s}_v}{\bar{s}_v}, \tag{17}$$

where s_v is virtual static energy. The non-hydrostatic pressure is ignored, both in its gradient acceleration and in its contributions to the density variations: in this model vertical accelerations are related entirely to (virtual) temperature-induced buoyancy perturbations, on the scale of the clouds. This excludes potentially important pressure effects (Holton, 1973; Yau, 1979); examination of the steady state, however, would filter out the growth-rate effects even with pressure included. Moreover, pressure has not appeared in the problem (the horizontal momentum equations not being used) and its introduction here would only require further closure. In any case, pressure effects for the shallow clouds studied here are small.

The momentum balance (17) can be horizontally averaged exactly like the moist static energy budget was previously [the results being (10a, b)]. However, the in-cloud momentum is not well-mixed and the cloud-mean vertical advection must be retained.

The problem of turbulence closure arises here exactly as it did in the discussion of the in-cloud budget of moist static energy (7). A first-order closure, with attendant uncertainty in the prescribed mixing length, would give turbulence contributions to (17) only if the eddy viscosity were not constant with height (since $\partial \bar{w}^c/\partial z$ is constant with height, by assumptions). The model here is formulated with the overall philosophy of adopting the simplest possible approach, and higher order closures are avoided whenever a less complex closure is physically reasonable. Both numerical (Sommeria, 1976) and experimental (e.g., Warner, 1970) studies of vertical velocity distributions in trade-wind cumulus conditions show that the dominant contributions to the vertical velocity power spectra arise from scales on the order of the cloud-cell size. Warner's (1970) experimental data also show a contribution from smaller scales, with the high wavenumber energy decreasing somewhat more rapidly than would be expected for a non-viscous turbulence cascade. Therefore, it is hypothesized here that the small-scale vertical velocity turbulence energy in the clouds is effectively separate from the cloud-mean motions, and the latter are not explicitly affected either by dissipation or the former. Thus, the overturning is forced exclusively by buoyancy perturbations on the cloud scale and does not interact with the smaller scales.

With these assumptions, the derivatives in (17) expand to be

$$\frac{d\bar{w}^c}{dt} = \bar{w}^c \frac{\partial \bar{w}^c}{\partial z} + \bar{E}^c(\bar{w}^c - \bar{w}^e), \tag{18a}$$

$$\frac{d\bar{w}^e}{dt} = \bar{w}^e \frac{\partial \bar{w}^e}{\partial z} - \bar{D}\mu(\bar{w}^c - \bar{w}^e). \tag{18b}$$

The overturning constitutes a direct circulation, and the closure is obtained via a circulation integral, upward through the clouds and downward through the environment. The horizontal legs of the integral are ignored, in keeping with the neglect of pressure variations. The buoyancy forcing of the circulation is

$$B \equiv g \int_0^1 \frac{\bar{s}_v^c - \bar{s}_v^e}{\bar{s}_v} d\hat{z}. \tag{19}$$

Taking the circulation integral, using (18a) and (18b) and substantial algebra yields

$$(\alpha - z_C/z_B)[\zeta - (2 - 3\sigma)(\alpha - z_C/z_B)] = 2(z_B - z_C)\left(\frac{\sigma}{\bar{w}_B}\right)^2 B, \tag{20}$$

where

$$\zeta \equiv 2\sigma z_C/z_B + \mu(1 - z_C/z_B).$$

Since the overturning can only be with $\alpha \geq z_C/z_B$ (clouds up), the root $\alpha = z_C/z_B$ is used whenever $B \leq 0$.

The virtual static energies are related to h and r by linearization (e.g., Randall, 1980b):

$$\bar{s}_v^c - \bar{s}_v^e = \bar{s}_{v_C}^c + \Gamma_v(z - z_C) + (\Delta h - (1 - \delta\epsilon)L\Delta r) - (\bar{h}^c - (1 - \delta\epsilon)L\bar{r}^c) \tag{21}$$

where $\delta = 0.608$ and $\epsilon = c_p T/L$. In (21) the fourth right-side term is an artificial "dry" cloud-base moist static energy which cancels part of the third term; the actual cloud profile is linearized and is given by the first two right-side terms, where

$$\Gamma_v \equiv g(1 - \beta)[1 - (1 + \delta)\epsilon],$$

is analogous to the lapse rate, and

$$\beta \equiv \frac{1 + (1 + \delta)\gamma\epsilon}{1 + \gamma}; \quad \gamma = \frac{L}{c_p}\frac{\partial q^*}{\partial T}\Big)_p$$

with q^* representing saturated specific humidity. The linearization of $\bar{s}_v^c$ allows the liquid water to increase upward and the temperature and water vapor to decrease upward. The difference between the first and last right-side terms in (21) is related to the cloud-base liquid water content:

$$\bar{s}_{v_C}^c - [\bar{h}^c - (1 - \delta\epsilon)L\bar{r}^c] = [1 - (1 + \delta)\epsilon]L\bar{l}_C^c.$$

For the cloud to exist, of course, $\bar{l}_C^c > 0$; this constraint will be used in the next section to find a maximum entrainment rate. That the in-cloud virtual static energy is greater than the "dry" value is purely a result of the linearization introduced in (21).

One qualitative analysis is of interest. Defining a vertically averaged cloud environment virtual temperature difference

$$\langle \Delta T_v \rangle \equiv \frac{s_{vr}}{gc_p} B,$$

where the denominator of (19) has been replaced by a reference value (s_{vr}) the right side of (20) becomes

$$2(z_B - z_C)(\sigma/\bar{w}_B)^2 g c_p/s_{vr}\langle \Delta T_v \rangle.$$

For the suppressed conditions during ATEX, the terms multiplying $\langle \Delta T_v \rangle$ are $O(10^8)$. The left-hand terms in (20), meanwhile, each turn out to be $O(10^2)$ at most. Hence $\langle \Delta T_v \rangle$ is quite small, $O(10^{-4})$.

Esbensen's (1978) diagnostic study of low clouds also found small values of $\langle \Delta T_v \rangle$, $O(10^{-1})$, using an entirely different approach from the present study not including cloud-top overshooting [i.e., $\Delta T_v(z) > 0$ everywhere]. The overshooting in the present model produces a region just below z_B where $\Delta T_v(z) < 0$; this tends to cancel most of the positive area lower down, and the vertical average is smaller. Albrecht *et al.* (1979) specified $\langle \Delta T_v \rangle$ in a closure for $\bar{E}^c$ and found little difference in their model for $\langle \Delta T_v \rangle = 0.0, 0.5$ K. The very low values obtained

TABLE 1. Model input quantities and sources.

Quantity	Value	Source
Fractional cloud area	$\sigma = 0.5$	1, 2
Large-scale divergence	$\bar{D} = 5.7 \times 10^{-6}\ s^{-1}$	2
Moist static energy above PBL	$h_u = 322.3\ kJ\ kg^{-1}$	1
Water vapor above PBL	$r_u = 0.0052$	1
Height of PBL	$z_B = 1650\ m$	1
Height of cloud base	$z_C = 800\ m$	1
Environmental cooling due to radiation	$\frac{1}{\rho c_p}\frac{\partial \bar{F}_R^e}{\partial z} = 3.2\ K\ day^{-1}$	2
In-cloud cooling due to radiation	$\frac{1}{\rho c_p}\frac{\partial \bar{F}_R^c}{\partial z} = 0$	2
Cloud-top radiative flux	$\rho \Delta F_R^{ct} = 100\ W\ m^{-2}$	2
Precipitation flux	$\bar{F}_P^c = 0$	1
Cooling by temperature advection	$\bar{\mathbf{V}} \cdot \overline{\nabla T} = 1.7\ K\ day^{-1}$	3, 1
Drying by moisture advection	$\bar{\mathbf{V}} \cdot \overline{\nabla q} = 0$	(text)
Cloud-base sensible heat flux	$\rho c_p \overline{w' T_C'} = -25\ W\ m^{-2}$	1
Cloud-base latent heat flux	$\rho L \overline{w' q_C'} = 150\ W\ m^{-2}$	1

Sources:
1. Augstein *et al.* (1973).
2. Albrecht *et al.* (1979).
3. Schaller and Kraus (1978).

by the scaling above reflect the high efficiency of the cloud-scale motions, the small-scale turbulence and any dissipation having been ignored for the overturning mechanism.

4. Results

This paper is concerned only with the mechanics of vertical mixing by PBL clouds and the model is incomplete in that cloud-base fluxes and the layer geometry must be prescribed. Large-scale "observations" of the fluxes are not obtained directly, but come either as budget residuals (e.g., Augstein *et. al.*, 1973) or from more complete model simulations (e.g., Albrecht *et al.*, 1979). Rather than attempt a wide range of calculations using arbitrarily varying data, the procedure here is to present model solutions for one set of conditions and discuss model results for two extremes of entrainment. Table 1 shows input parameters, values and sources. The cloud-base sensible heat flux is perhaps low compared to the moisture flux, but this can be resolved only with a complete PBL model. Large-scale moisture advection and precipitation have been neglected. The assumption in the present model that the clouds are vertically well mixed implies that the value $\sigma = 0.5$ is an overestimate (half the large-scale area is well mixed) but this value will be retained. The only necessary input parameter which is not available is the entrainment (or the detrainment).

The model was solved using Table 1 conditions and specified values of $\bar{D}^c/\bar{D}$. This was accomplished by guessing α, solving the budget equations and using the resultant profiles of h and r to calculate B via (19) and (21). The residual of (20) was then minimized using a *regula falsi* iteration, with convergence at the 0.1% level. Fig. 2 shows variation of $(\bar{E}^c/\bar{D})$, $\langle \Delta T_v \rangle$, and α for the range of $\bar{D}^c/\bar{D}$ which produces physically reasonable results. For $\bar{D}^c/\bar{D} \geqslant 25$ the calculated entrainment rate becomes negative, and for $\bar{D}^c/\bar{D} \leqslant 10.5$ the cloud-base liquid water content becomes "negative" (i.e., $\bar{r}_C^c < \bar{q}_C^{*c}$). The physical links for these cut-offs are straightforward. In the low $\bar{D}^c/\bar{D}$ case, the high entrainment rate is associated with a relatively diluted cloud, small buoyancy and cloud-base vertical velocity. In this case, the cloud is "diluted" in the sense that the input of dry environmental air from the sides, by entrainment, is as large as it can be while maintaining enough moisture for condensation at cloud base. Despite the assumption that the cloud is well mixed, the cloud moisture is lower than the zero-entrainment limit. In that latter limit, which is "undiluted" by the above reasoning, the buoyancy and cloud-base updrafts are large. This nomenclature will be continued in the following discussion.

Fig. 3 shows vertical profiles of $\bar{h}$, $\bar{q}$ and $\bar{T}$ for the diluted (solid) and undiluted (dashed) cases and $\bar{h}^e$, $\bar{q}^e$, $\bar{T}^e$ for the diluted case, along with ATEX profiles from Augstein *et al.* (1973). The diluted and undiluted cases differ mostly in the upper part of the layer—the inversion—and these differences are consistent with the previous discussion of Fig. 1. The forcing in Table 1 produces reasonable agree-

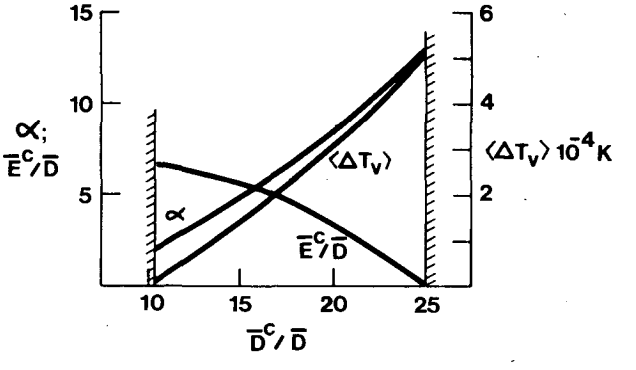

FIG. 2. Model entrainment (normalized by large-scale divergence) and overturning (left scale) and vertically averaged cloud-environment virtual temperature difference versus normalized cloud detrainment (specified).

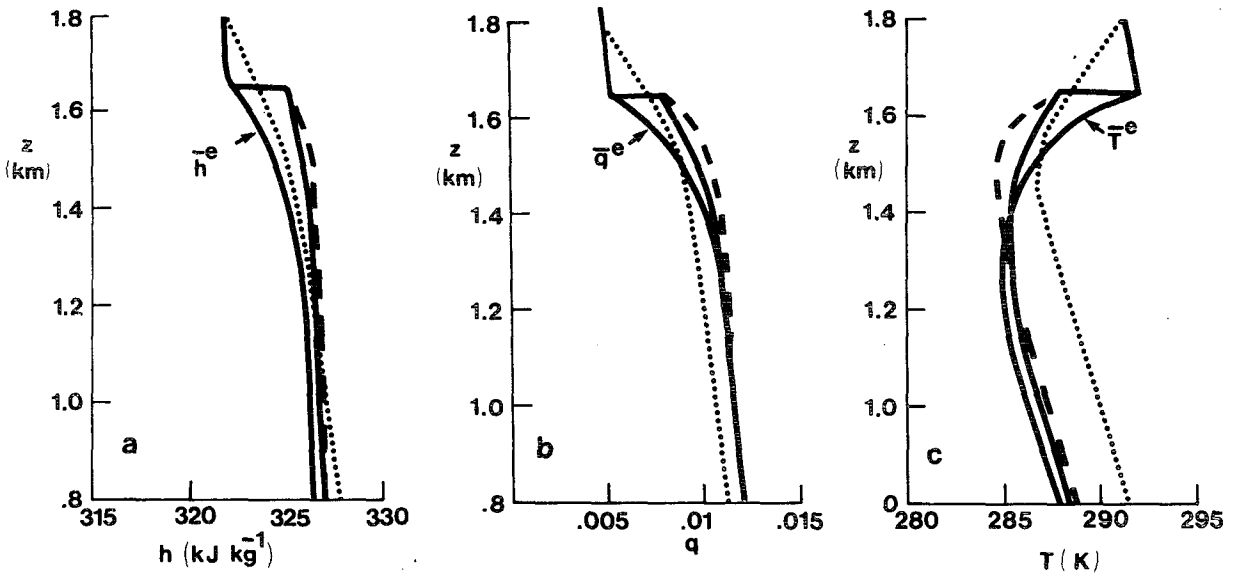

FIG. 3. Vertical profiles of moist static energy (a), water vapor (b), and temperature (c) for ATEX (dotted), zero entraiment (dashed) and maximum entrainment (solid).

ment for the moist static energy profiles (Fig. 3a), but neglecting large-scale moisture advection overpredicts the layer water vapor (Fig. 3b). The temperature profiles are low by ~2.5 K near cloud base; this is in compensation for the ~1 g kg^{-1} water vapor overprediction [i.e., $L/c_p(0.001) \sim 2.5$ K]. In both the undiluted and diluted cases, the inversion is much more stable (i.e., it is sharper) than the ATEX observations; this is a result of having assumed the clouds (half the large-scale area here) to be well mixed and is clearly evident in the flux profiles discussed below.

Fig. 4 shows the sub-large-scale fluxes of the conserved variables ($s_l = h - Lr$) for the two cases. Again, the undiluted case (dashed) shows the sharper inversion characteristic of large μ and α. The $\overline{w's_l'}$ curves exhibit cooling in the upper part of the layer and warming lower down where vertical advection (i.e., subsidence warming) dominates cooling effects by detrainment (Betts, 1975). At all levels, the moist static energy and total water fluxes converge with largest additions of these quantities to the upper part of the layer. The breakdown of the liquid static energy fluxes [$\overline{w's_l'}$ components from (1b)] in Fig. 5 is remarkable, because the roles of the two mixing processes have nearly reversed. Since the entrainment is zero for the undiluted case, the small-scale flux $\sigma\overline{w's_l'}^c$ is linear with height (curve d); it is, moreover, completely dominated by the overturning (curve c). For the diluted case, the overturning (curve a) is relatively weak (α is small: see Fig. 2), while the small-scale flux (curve b) exhibits strong curvature due to the large $\bar{E}^c$ [see Eq. (14)]. Comparing the two cases in both Figs. 4 and 5 reveals that the diluted clouds cool a larger fraction of the layer than the undiluted clouds despite the larger detrainment of the latter. This is due to the much stronger overturning in the undiluted case and, consequently, stronger subsidence warming. These are precisely the differences between deep and shallow cumuli revealed by spectral budget studies (Yanai *et al.*, 1976).

The cloud base updraft strength for the two cases is ~0.01 m s^{-1} (diluted) and ~0.11 m s^{-1} (undiluted); if, as suggested by Augstein *et al.* (1973) only 2%

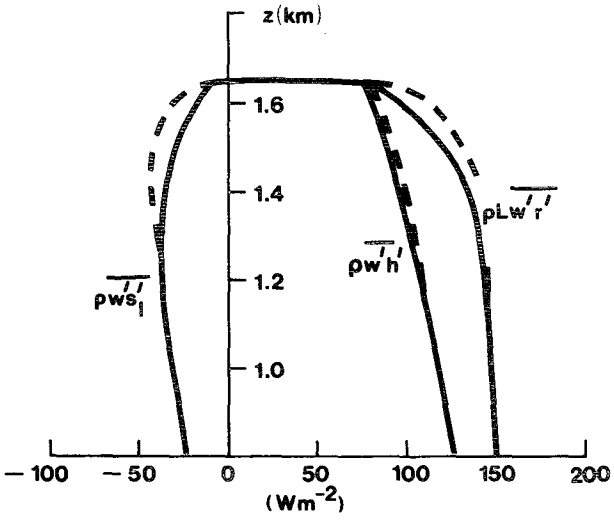

FIG. 4. Model vertical subgrid fluxes of total water in energy units ($\rho L\overline{w'r'}$), moist static energy ($\rho\overline{w'h'}$) and liquid static energy ($\rho\overline{w's_l'}$). Solid curves are for maximum entrainment and dashed for zero entrainment.

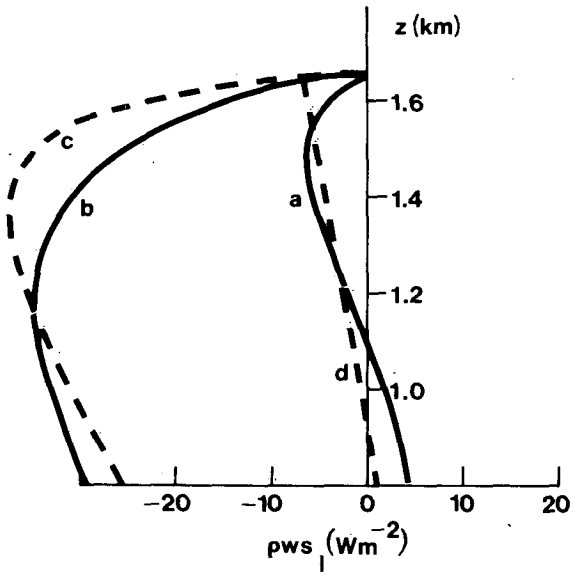

FIG. 5. Breakdown of liquid static energy fluxes for the two cases. Curves a and c represent the overturning component $[\sigma(1-\sigma)\rho(\bar{w}^c-\bar{w}^e)\Delta s_l]$ and curves b and d show the small-scale in-cloud component $(\sigma\rho\overline{w's_l'}^c)$. Solid curves for maximum entrainment, dashed for zero entrainment.

of the clouds are responsible for the active updrafts, these become 0.5 and 5.5 m s^{-1}, respectively. These bracket the value (of ~1 m s^{-1}) inferred by Augstein *et al.* (1973) with the diluted case here being closer to the ATEX value. This is consistent with the profiles in Fig. 3. For both cases, the net cloud-base flux is identical, being prescribed; Eq. (15a) shows that the model adjusts to partition this into the overturning scale and the subcloud scale. The diluted case corresponds to large amounts of subcloud-scale energy and the undiluted case to large amounts of cloud-scale energy. Since deep cumuli are relatively undiluted (i.e., the "hot tower" of Riehl and Malkus, 1958) it is concluded that shallow diluted clouds are associated mostly with small-scale fluxes, and deeper undiluted clouds are associated with the overturning mechanism. This conclusion, of course, is tentative because both cases here have the same geometry. In this context, it must be asked whether the undiluted clouds have the potential for deeper growth. If so, the conclusion above is fortified. Fig. 6 shows the virtual static energy (buoyancy) fluxes for the two cases. The greater strength of the overturning for the undiluted case is obvious. The vertical integral of the buoyancy fluxes is proportional to the kinetic energy generated by the cloud processes, and that by the undiluted clouds is clearly larger in Fig. 6. Therefore, the undiluted clouds have the potential to grow upward farther than the diluted clouds.

5. Conclusion

a. Summary

A simplified model of the undisturbed trade-wind cloud/inversion layer has been presented which yields analytic solutions for the budgets of moist static energy and total water, and a quasi-analytic solution for the cloud-base vertical velocities. Since

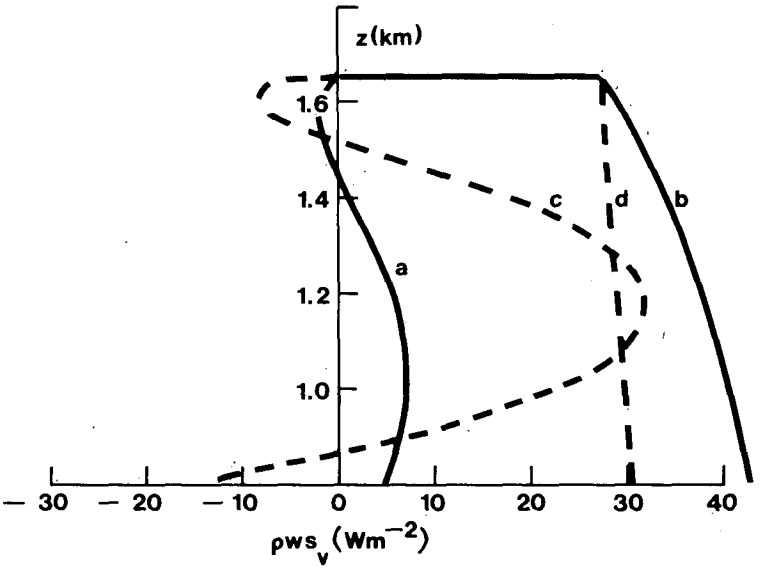

FIG. 6. Breakdown of virtual static energy (buoyancy) fluxes. Curves a and c represent the overturning component $[\sigma(1-\sigma)\rho(\bar{w}^c-\bar{w}^e)\Delta s_v]$ and curves b and d show the small-scale in-cloud component $(\sigma\rho\overline{w's_v'}^c)$. Solid curves for maximum entrainment, dashed for zero entrainment.

a model of the surface, subcloud and transition layers is not included, cloud-base fluxes and layer geometry must be specified, and this limits application of the model to examination of the cloud mixing processes.

The analytic solutions are possible because a number of quantities are assumed constant with height: the cloud area, the large-scale divergence and advection, the cloud entrainment and detrainment, the radiative forcing and the in-cloud moist static energy and total water. In addition, small-scale turbulence is neglected in the environment and the vertical velocities are associated only with buoyancy perturbations (pressure perturbations are neglected).

The main contribution made here is the inclusion of two mechanisms for cloud-related mixing, the in-cloud small-scale turbulence and the overturning which is associated with the saturated updrafts in the clouds and unsaturated downdrafts between them. Despite the many simplifications, the model produces reasonable agreement with ATEX profiles, although results are strongly biased by the assumption of well-mixed clouds.

No attempt has been made here to parameterize the cloud entrainment; consequently either it or the cloud detrainment must be specified. Calculations show, for conditions corresponding to the ATEX situation, that two extremes of entrainment (one zero, one the maximum which maintains a saturated cloud base) produce dramatically different contributions from the two mixing processes. It has been argued that the undiluted case (entrainment zero) corresponds to the mechanisms associated with deep, energetic cumulus for which the overturning dominates. The maximum entrainment case seems to correspond more nearly to the shallow PBL clouds responsible for moistening and cooling the trade wind cloud and inversion layers.

b. Discussion

Two topics are discussed here: model improvement and extensions, and implications of modeled processes for the tropical circulation.

The most restrictive assumption used in this formulation is that the clouds are well-mixed. One model improvement was discussed in Section 2, introducing two types of clouds, growing and decaying, with only the growing clouds taken as well mixed. Another possibility would be to retain the two sublarge-scale averaging areas (clouds and environment) and relax the well-mixed assumption by allowing a linear cloud stratification (making the subcloud-scale flux quadratic in the undiluted case). This approach would decrease the cloud-top "jumps" and would require only one further closure assumption. Albrecht *et al.* (1979) showed solutions to such an approach with closure for the entrainment rate but without the in-cloud turbulence.

Given the results discussed above concerning the differences between the diluted and undiluted clouds, it is useful to examine the implications for a closure on the entrainment rate $\bar{E}^c$. The classic approach for cloud models takes a lateral entrainment length scale to be equal to the logarithmic rate of increase for the cloud mass flux M, i.e.,

$$\lambda = \frac{1}{M}\frac{dM}{dz}$$

(e.g., Betts, 1973). A vertically averaged entrainment length scale can be deduced from the present model results by taking

$$\langle\lambda\rangle = \bar{E}^c/\langle\bar{w}^c\rangle.$$

For the undiluted case, $\bar{E}^c = 0$, the entrainment length is infinite (i.e., $\lambda = 0$). The results closest to ATEX conditions (for a 2% updraft area cloud velocity of $\sim$1 m s^{-1}) gives an entrainment scale of about 200 m, and the diluted case discussed in Section 4 has $\lambda \sim (10\text{ m})^{-1}$. This clearly shows that more diluted clouds are associated with smaller lateral entrainment length scales, which is physically consistent with the increasing dominance of the subcloud-scale mixing for diluted cases.

One further analysis is of interest, using results from an unreported sensitivity experiment for which Table 1 conditions were applied to the model with the exception that the cloud base moisture flux (and moist static energy flux) was increased by the equivalent of 5 W m^{-2}. In terms of the idealized tropical circulation this corresponds to a small downstream displacement toward warmer water, with larger vapor pressure and fluxes (Arakawa, 1975; Schubert, 1976). In this case, the physically realistic values of $\bar{D}^c/\bar{D}$ (Fig. 2) are displaced toward the left (lower $\bar{D}^c/\bar{D}$), corresponding to clouds with longer lifetimes. Also, the values of entrainment lie below those in Fig. 2, indicating that clouds with the same $\bar{D}^c/\bar{D}$ are less diluted as the energy flux into the bases is increased. Qualitatively, then, the evolution of PBL clouds along trajectories in the trades can be viewed as an increase in the scales of motion associated with vertical mixing as the ocean becomes warmer and more energy is available for mixing against the stable, descending air above the PBL. Corresponding to this increase in convective scales are less lateral cloud entrainment and the potential for deeper cloud growth. This is in general agreement with observations of the evolving trade-wind PBL.

Because the model presented here is confined to the mixing processes within the cloud and inversion layers, several quantities which are dependent on other PBL processes were specified; these include the cloud base and top heights, the cloud-base fluxes, the cloud area and the radiative cooling rates. The

cloud-base fluxes and height could be found by inclusion of surface, subcloud and transition layer models. The latter, in particular, is difficult because the various types of clouds of interest are associated with different transition layer physics (Arakawa and Schubert, 1974; Betts, 1976). The cloud-top height could be found from a closure on the turbulence budget, as in stratocumulus models. Albrecht (1981) has recently proposed a parameterization to find the cloud area. With such extension, the present model can be used to study the evolving PBL discussed in the Introduction.

Acknowledgments. This study was begun as a doctoral research project at the Rosenstiel School of Marine and Atmospheric Sciences, University of Miami, supported by National Science Foundation Grants ATM75-22940 and ATM77-28126, with Prof. E. B. Kraus, advisor. L. H. Lahiff provided a most useful review of the manuscript, and anonymous reviewers' comments were very helpful for clarity in revision. I also thank Ann Tankard for her patience with the typing.

REFERENCES

Albrecht, B. A., 1979: A model of the thermodynamic structure of the trade-wind boundary layer: Part II. Applications. *J. Atmos. Sci.*, **36,** 90–98.

——, 1981: Parameterization of trade-cumulus cloud amounts. *J. Atmos. Sci.*, **38,** 97–105.

——, A. K. Betts, W. H. Schubert and S. K. Cox, 1979: A model of the structure of the trade-wind boundary layer: Part I. Theoretical formulation and sensitivity tests. *J. Atmos. Sci.*, **36,** 73–89.

Arakawa, A., 1975: Modelling of clouds and cloud processes for use in climate models. *Physical Basis of Climate and Climate Modelling, GARP Publ. Ser.*, No. 16, WMO/ICSU JOC (see Appendix 4).

——, and W. H. Schubert, 1974: Interaction of a cumulus cloud ensemble with the large-scale environment. Part I. *J. Atmos. Sci.*, **31,** 674–701.

Augstein, E., H. Riehl, F. Ostapoff and V. Wagner, 1973: Mass and energy transports in an undisturbed trade-wind flow. *Mon. Wea. Rev.*, **101,** 101–111.

——, M. Garstang and G. D. Emmitt, 1979: Vertical mass and energy transports by cumulus clouds in the tropics. *Deep-Sea Res.*, **26**(GATE Suppl. I), 9–21.

Betts, A. K., 1973: Non-precipitating cumulus convection and its parameterization. *Quart. J. Roy. Meteor. Soc.*, **99,** 178–196.

——, 1975: Parametric interpretation of trade-wind cumulus budget studies. *J. Atmos. Sci.*, **32,** 1934–1945.

——, 1976: Modeling subcloud layer structure and interaction with a shallow cumulus layer. *J. Atmos. Sci.*, **33,** 2363–2382.

Deardorff, J. W., 1976a: On the entrainment rate of a stratocumulus topped mixed layer. *Quart. J. Roy. Meteor. Soc.*, **102,** 563–582.

——, 1976b: Usefulness of liquid-water potential temperature in a shallow cloud model. *J. Appl. Meteor.*, **15,** 98–102.

——, 1980: Cloud-top entrainment instability. *J. Atmos. Sci.*, **37,** 131–147.

——, and J. A. Businger, 1980: Comments on "Marine stratocumulus convection. Part I: Governing equations and horizontally homogeneous solutions." *J. Atmos. Sci.*, **37,** 481–482.

Esbensen, S., 1978: Bulk thermodynamic effects and properties of small tropical cumuli. *J. Atmos. Sci.*, **35,** 826–837.

Holton, J. R., 1973: A one-dimensional cumulus model including pressure perturbations. *Mon. Wea. Rev.*, **101,** 201–205.

Kahn, P. H., and J. A. Businger, 1979: The effect of radiative flux divergence on entrainment of a saturated convective boundary layer. *Quart. J. Roy. Meteor. Soc.*, **105,** 303–306.

LeMone, M. A., and W. T. Pennell, 1976: The relationship of trade-wind cumulus distribution to subcloud layer fluxes and structure. *Mon. Wea. Rev.*, **104,** 524–539.

Lilly, D. K., 1968: Models of cloud-topped mixed layers under a strong inversion. *Quart. J. Roy. Meteor. Soc.*, **94,** 292–309.

——, and W. H. Schubert, 1980: The effects of radiative cooling in a cloud-topped mixed layer. *J. Atmos. Sci.*, **37,** 482–487.

Mellor, G. L., and T. Yamada, 1974: A hierarchy of turbulence closure models for planetary boundary layers. *J. Atmos. Sci.*, **31,** 1791–1806.

Niiler, P. P., and E. B. Kraus, 1977: One-dimensional models of the upper ocean. *Modelling and Prediction of the Upper Layers of the Ocean*, E. B. Kraus, Ed., Pergamon Press, 143–172.

Nitta, T., 1975: Observational determination of cloud mass flux distributions. *J. Atmos. Sci.*, **32,** 73–91.

Ooyama, K., 1971: A theory on parameterization of cumulus convection. *J. Meteor. Soc. Japan*, **49**(Special Issue), 744–756.

Randall, D. A., 1980a: Conditional instability of the first kind upside-down. *J. Atmos. Sci.*, **37,** 125–130.

——, 1980b: Entrainment into a stratocumulus layer with distributed radiative cooling. *J. Atmos. Sci.*, **37,** 148–159.

Riehl, H., and J. S. Malkus, 1958: On the heat balance of the equatorial trough zone. *Geophysica*, **6,** 503–538.

——, J. M. Simpson, 1979: The heat balance of the equatorial trough zone, revisited. *Contrib. Atmos. Phys.*, **52,** 287–305.

Schaller, E., and H. Kraus, 1978: Time-dependent inversions in different climatic regions. *Contrib. Atmos. Phys.*, **51,** 230–246.

Schubert, W. H., 1976: Experiments with Lilly's cloud-topped mixed-layer model. *J. Atmos. Sci.*, **33,** 436–446.

——, J. S. Wakefield, E. J. Steiner and S. K. Cox, 1979: Marine stratocumulus convection. Part I: Governing equations and horizontally homogeneous solutions. *J. Atmos. Sci.*, **36,** 1286–1324.

Sommeria, G., 1976: Three-dimensional simulation of turbulent processes in an undisturbed trade-wind boundary layer. *J. Atmos. Sci.*, **33,** 216–241.

Warner, J., 1980: The microstructure of cumulus cloud. Part III. The nature of the updraft. *J. Atmos. Sci.*, **27,** 682–688.

——, 1977: Time variation of updraft and water content in small cumulus clouds. *J. Atmos. Sci.*, **34,** 1306–1312.

Winston, J. S., A. Gruber, T. I. Gray, Jr., M. S. Varnadore, C. L. Earnest and L. P. Mannelo, 1979: *Earth-Atmosphere Radiation Budget Analyses Derived from NOAA Satellite Data June 1974–February 1978*, Vol. 1. Meteorological Satellite Laboratory, NOAA/NESS. U.S. Dept. of Commerce, Washington.

Yanai, M., S. Esbensen and J. H. Chu, 1973: Determination of bulk properties of tropical cloud clusters from large-scale heat and moisture budgets. *J. Atmos. Sci.*, **30,** 611–627.

——, J. H. Chu, T. E. Stark and T. Nitta, 1976: Response of deep and shallow tropical marine cumuli to large-scale processes. *J. Atmos. Sci.*, **33,** 976–991.

Yau, M. K., 1979: Perturbation pressure and cumulus convection. *J. Atmos. Sci.*, **36,** 690–694.